

Creating entanglement using integrals of motion

Maxim Olshani, ^{1,*} Thibault Scoquart, ^{2,1} Dmitry Yampolsky, ¹ Vanja Dunjko, ^{1,†} and Steven Glenn Jackson ³

¹*Department of Physics, University of Massachusetts Boston, Boston, Massachusetts 02125, USA*

²*Département de Physique, Ecole Normale Supérieure, 24, rue Lhomond, 75005 Paris, France*

³*Department of Mathematics, University of Massachusetts Boston, Boston, Massachusetts 02125, USA*



(Received 5 October 2016; revised manuscript received 10 January 2017; published 26 January 2018)

A quantum Galilean cannon is a one-dimensional sequence of N hard-core particles with special mass ratios and a hard wall; conservation laws due to the reflection group A_N prevent both classical stochastization and quantum diffraction. It is realizable through specie-alternating mutually repulsive bosonic soliton trains. We show that an initial disentangled state can evolve into one where the heavy and light particles are entangled, and we propose a sensor, containing N_{total} atoms, with a $\sqrt{N_{\text{total}}}$ times higher sensitivity than in a one-atom sensor with N_{total} repetitions.

DOI: [10.1103/PhysRevA.97.013630](https://doi.org/10.1103/PhysRevA.97.013630)

I. INTRODUCTION

In a one-dimensional (1D) system of hard-core particles, by tuning the ratios between the particle masses one can choose a variety of distinct regimes of motion [1,2]. While generic values result in thermalization, for some special ones the system maps to known multidimensional kaleidoscopes [3,4]. The outcome velocities then become determined by the initial velocities only, independent of the initial positions if the particle ordering is preserved. In the quantum version, the eigenstates are finite superpositions of plane waves, with no diffraction [5]. In particular a (run in reverse) Galilean cannon—a hard wall followed by a 1D sequence of N hard-core particles with mass ratios of $1 : \frac{1}{3} : \frac{1}{6} : \frac{1}{10} : \dots : \frac{2}{N(N+1)}$ —will evolve from a state where only the lightest particle is moving (approaching the others from infinity), to a state where all of the particles are moving away from the wall, with the same speeds. The final state of the heavy particles is very different from the initial one, yet highly predictable, presenting an opportunity: if created, a superposition of the final and initial states would resemble a Schrödinger cat state [6], in the following sense: just as the α particle controls the well-being of the cat, so the state of the lightest particle controls either (a) the rest of the particles or (b) the heaviest particle, after the others are detected [7]. And yet the whole system is in a pure state. The stored entanglement is ready to be used, and we will propose an interferometric application.

II. GENERAL SOLUTION FOR A TIME-DEPENDENT SCHRÖDINGER EQUATION FOR A GALILEAN CANNON ENSEMBLE OF HARD-CORE PARTICLES: EXAMPLE OF A GAUSSIAN INITIAL STATE

Consider a system of N 1D hard-core particles with masses m_1, m_2, \dots, m_N on the half line $x > 0$, bounded by a hard

wall at $x = 0$. The Hamiltonian is given by the kinetic energy,

$$\hat{H} = - \sum_{i=1}^N \frac{\hbar^2}{2m_i} \frac{\partial^2}{\partial x_i^2}; \quad (1)$$

the wave function $\Psi(x_1, x_2, \dots, x_N)$ satisfies the boundary conditions

$$\Psi|_{x_1=0} = \Psi|_{x_1=x_2} = \dots = \Psi|_{x_{N-1}=x_N} = 0. \quad (2)$$

The coordinate transformation $x_i = \sqrt{\mu/m_i} z_i$ for $i = 1, 2, \dots, N$, where μ is an arbitrary mass scale that can be chosen at will, converts the system to a single N -dimensional particle of mass μ moving inside a mirror-walled wedge formed by N mirrors; the outward normalized normals to its mirrors are given by $\mathbf{n}_1 = -\mathbf{e}_1$ and $\mathbf{n}_i = \sqrt{m_i/(m_{i-1} + m_i)}\mathbf{e}_{i-1} - \sqrt{m_{i-1}/(m_{i-1} + m_i)}\mathbf{e}_i$ for $i = 2, 3, \dots, N$, where \mathbf{e}_i is the unit vector along the z_i axis.

For a generic set of masses, sequential reflections about the mirrors generate an infinite set of spatial transformations. However, for every full reflection group [8] of a regular multidimensional polyhedron (i.e., Platonic solid), there is a set of masses whose corresponding system of mirrors generates that group [4]. In these cases the eigenstates of the system can be found exactly through Bethe ansatz [3,4]: they are given by finite linear combinations of plane waves. In particular, the “Galilean cannon” set of masses $m_1, m_2 = m_1/3, m_3 = m_1/6, \dots, m_N = \frac{2}{N(N+1)}m_1$ corresponds to the symmetry group of a regular N -dimensional tetrahedron [9].

As the initial state for the reverse Galilean cannon (Fig. 1, insert), we take the tensor product of the Gaussian wave packets for each particle, supplemented by its images needed to satisfy the boundary conditions (2). The corresponding solution of the time-dependent Schrödinger equation with the Hamiltonian (1), subject to the boundary conditions (2), is

$$\begin{aligned} & \Psi(z_1, z_2, \dots, z_N) \\ &= \left[\sum_{\hat{g}} (-1)^{P(\hat{g})} \hat{g} \right] \prod_{i=1}^N \psi(z_i, t | z_i^{(0)}, v_{z,i}, \sigma_{z,i}), \quad (3) \end{aligned}$$

*Maxim.Olchanyi@umb.edu

†Vanja.Dunjko@umb.edu

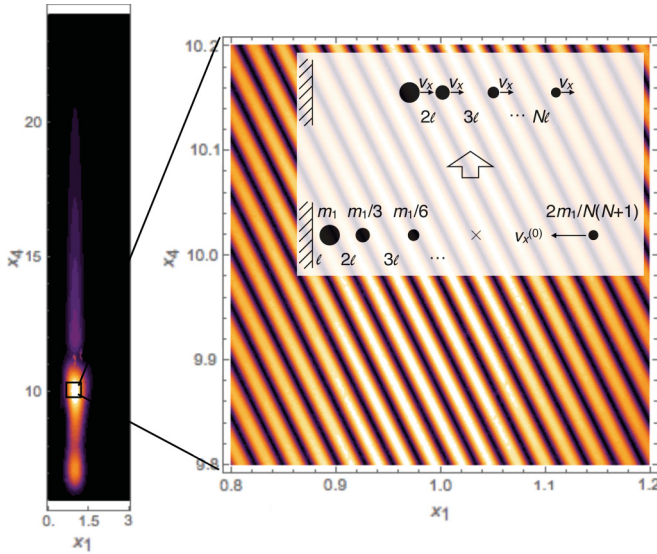


FIG. 1. A light-heavy entangled state produced in a Galilean cannon system with $N = 4$ particles. The conditional two-body density distribution for the heaviest and the lightest particles, $|\Psi(x_1, 3\ell, 6\ell, x_4)|^2$, is plotted, at a time t_{obs} , subject to the second and the third particles being held at $(x_2, x_3) = (3, 6)\ell$. The initial state is a Gaussian wave packet for each of the particles. The mean initial velocities of all the particles but the lightest vanish, while the lightest is approaching the system at a speed $\mathcal{V}_x^{(0)}$. The magnified portions are centered around the self-crossing point, $(x_1, x_2, x_3, x_4) = (1, 3, 6, 10)\ell$, where the head of the distribution is capable of crossing its tail. In the figures, the head part is not visible outside of the crossing with the tail. The centers of the initial Gaussians are at $(x_1^{(0)}, x_2^{(0)}, x_3^{(0)}, x_4^{(0)}) = (1, 3, 6, 31.5)\ell$. The speed $\mathcal{V}_x^{(0)}$, the observation time, and the dispersions of the initial Gaussians are $\mathcal{V}_x^{(0)} = 949\hbar/(m_1\ell)$, $t_{\text{obs}} = 0.0332 m_1 \ell^2/\hbar$, and $(\sigma_{x,1}, \sigma_{x,2}, \sigma_{x,3}, \sigma_{x,4}) = (0.129, 0.223, 0.315, 9.49)\ell$, respectively. With the exception of the lightest particle direction, the initial spatial distribution is round, if expressed through the z coordinates; it is disproportionately elongated in the z_4 direction (i.e., the initial state of the lightest particle is comparatively much broader) to ensure that the many-body wave packet can self-cross. The observation time corresponds to the exact middle point of the time evolution (see main text). Inset: Galilean cannon run in reverse: the lightest particle sets in motion all the heavy particles, at the same speed. In addition, the initial positions of the particles are chosen in such a way that there exists a particle configuration—namely, the initial positions of all particles but the lightest, whose position is instead indicated by the cross—that is realized *twice* in the course of the time evolution.

where

$$\Psi(z, t | z^{(0)}, v_z, \sigma_z) = A(t)e^{-\frac{(z-z^{(0)})^2 - 4i\hbar\mu\sigma_z^2 v_z(z-z^{(0)}) + 2i\mu v_z^2 \sigma_z^2 t/\hbar}{4\sigma_z^2[1 + (i\hbar t)/(2\mu\sigma_z^2)]}}$$

is the one-body Gaussian wave packet expanding freely; $A(t) = \{2\pi\sigma_z^2[1 + (i\hbar t)/(2\mu\sigma_z^2)]\}^{-1/4}$ is the normalization constant. The sum runs over all possible distinct orthogonal transformations of space \hat{g} : all possible distinct outcomes that can be generated by a finite succession of N reflections \hat{g}_{n_i} ,

$$\Psi(z) \xrightarrow{\hat{g}_{n_i}} \Psi(z - 2(n_i \cdot z)n),$$

about mirrors defined by the normals n_i described above. Each transformation \hat{g} can be labeled by a permutation of $N + 1$ objects with labels $0, 1, 2, \dots, N$; the N generators above are mapped to a permutation of two consecutive objects, $\hat{g}_{n_i} \rightarrow [(i - 1) \leftrightarrow i]$, and the multiplication table of the \hat{g} 's is identical to the multiplication table of the permutations. This solution is obtained in the same way as the Bethe eigenstates in the case of hard-wall kaleidoscopes [4], which, in turn, is a special case of the general solution for kaleidoscopes with Robin's boundary conditions [3, 10–15], which was inspired by the Bethe ansatz solutions for a gas of bosons [16–19]. The set of \hat{g} 's forms the reflection group A_N , containing $(N + 1)!$ elements [20]. $\mathcal{P}(\hat{g})$ is the parity of the group element, i.e., the parity of the number of reflections about the N generating mirrors (given in particular by the normals n_i above) needed to produce this element.

III. GENERATING AN ENTANGLED STATE USING LONG WAVE PACKETS

Having obtained the general solution for the problem, let us return to the physical coordinates x_1, x_2, \dots, x_N . For the sequence depicted in the inset of Fig. 1 (“the Galilean cannon run in reverse”), the initial velocities of the particles are $v_{x,N} = -\mathcal{V}_x^{(0)} < 0$ and $v_{x,1} = v_{x,2} = \dots = v_{x,N-1} = 0$. At the final stage of the process, each particle moves away from the wall with the same speed $\mathcal{V}_x = \sqrt{m_N/M}\mathcal{V}_x^{(0)} = \mathcal{V}_x^{(0)}/N$, where $M = \sum_{i=1}^N m_i$ is the total mass of the system. The initial distances between the particles, and between the leftmost particle and the wall, are assumed much greater than the widths of their initial packets: $x_1^{(0)} \gg \sigma_{x,1}$ and $x_i^{(0)} - x_{i-1}^{(0)} \gg \max(\sigma_{x,i}, \sigma_{x,i-1})$ for $i = 2, 3, \dots, N$. In this case, the initial state is close to a *product* state of individual nonoverlapping states of finite support: the images, while formally present in the expression (3), will be exponentially small at $t = 0$ (but will come to prominence at later times, as the particle wave packets move around and broaden).

If the initial multidimensional Gaussian wave packet is sufficiently long, the various parts of the superposition (3) will start overlapping at intermediate stages of the time evolution, forcing the particles to entangle—despite the closeness of the initial state to a product state. The most promising is the superposition between 1. the initial packet and 2. the “outgoing” one, where all the particles are moving with a velocity $+\mathcal{V}_x$: here the state of the lightest particle controls the state of each of the heavier ones, including the heaviest. It turns out that for a properly tuned set of initial conditions, there will be regions of space where these two waves *spatially overlap* and all other parts of (3) are exponentially small. Indeed, one can show that if a classical trajectory passes through the point $(x_1^{(\text{sc})}, x_2^{(\text{sc})}, \dots, x_N^{(\text{sc})}) = (\ell, 3\ell, 6\ell, \dots, \frac{N(N+1)}{2}\ell)$, it will do so *twice*, once during the initial leg of the evolution and once during the final. (Here and below, ℓ is an arbitrary length scale, and the subscript “sc” stands for “self-crossing.”) We will call $(x_1^{(\text{sc})}, x_2^{(\text{sc})}, \dots, x_N^{(\text{sc})})$ the “self-crossing point.” The distances between the particles increase linearly with the index: $x_j^{(\text{sc})} - x_{j-1}^{(\text{sc})} = j\ell$. At the exact middle point of the time evolution (which can be shown to equal the time when the lightest particle would hit the wall if there were no other

particles present), the state around the point of self-crossing is close to

$$\Psi(x_1, x_2, \dots, x_N) \propto e^{-i[m_N \mathcal{V}_x^{(0)}(x_N - x_N^{(sc)}) + \frac{\phi}{2}]} + e^{+i[\sum_{i=1}^{N-1} m_i \mathcal{V}_x(x_i - x_i^{(sc)}) + m_N \mathcal{V}_x(x_N - x_N^{(sc)}) + \frac{\phi}{2}]}, \quad (4)$$

where the relative phase ϕ can be approximated, using the eikonal approximation, as $\hbar\phi = 2m_1 \mathcal{V}_x^{(0)} \ell$. This is obtained from the classical action, $\int_{t^{(sc I)}}^{t^{(sc II)}} dt \sum_{i=1}^N m_i v_{x,i}^2(t)/2$, between the first and the second time the particles pass through the self-crossing point $(x_1^{(sc)}, x_2^{(sc)}, \dots, x_N^{(sc)})$. Here $v_{x,i}(t)$ is the classical trajectory with the initial coordinates and velocities given by the initial positions and velocities of the quantum Gaussian wave packets. In the state above, the coordinate of the lightest particle is entangled with the center-of-mass position of the remaining bodies. Below we will use this entanglement as a way to improve the sensitivity of interferometric measurements. As for the “cat” per se, we have the position of the center of mass of the particles being spread over an $\sim N^2 \ell$ range. If this seems too abstract, one can also generate entanglement between two localized objects, one light and one heavy: suppose the intermediate particles 2, 3, \dots , $N - 1$ have been detected at particular positions. The particles 1 and N remain entangled, in spite of the $N - 2$ hard walls between them formed by the detected intermediate particles. For example, when the intermediate particles are detected at their “self-crossing” values, the state of the system becomes

$$\Psi_{1,N}(x_1, x_N) \propto e^{-i[m_N \mathcal{V}_x^{(0)}(x_N - x_N^{(sc)}) + \frac{\phi}{2}]} + e^{+i[m_1 \mathcal{V}_x(x_1 - x_1^{(sc)}) + m_N \mathcal{V}_x(x_N - x_N^{(sc)}) + \frac{\phi}{2}]}. \quad (5)$$

This state resembles a paradigmatic Schrödinger cat state in the sense that a light particle (x_N), the “ α -particle,” is entangled with a heavy one (x_1), the “cat” [7].

Figure 1 shows the results of time propagation according to the above scheme, for $N = 4$. At the classical self-crossing point, the incident and the outgoing waves dominate: as a signature of that fact, we see the clear interference fringes in the x_1 - x_4 plane, with the wave vector given by the difference between the wave vectors of the two plane waves in (5). The absence of diffraction is a sign of integrability [5,18]. Also note that for a generic set of masses, the most probable outcome of the process is equipartition of energy. In this case, the velocity of the heaviest particle will be $\sqrt{N(N+1)/2} \stackrel{N \gg 1}{\approx} N$ times lower than in the integrable case, leaving it effectively at rest.

We have numerically computed the Rényi entropy $S_2[\text{particle 1}] = -\ln[\text{Tr}[\hat{\rho}_{\text{particle 1}}^2]]$ for the reduced density matrix $\hat{\rho}_{\text{particle 1}}$ of the heaviest particle, for the state truncated to the square area in Fig. 1, and (x_2, x_3) fixed to $(3, 6) \ell$. To compute the entropy, we discretized the (x_1, x_4) space into a square grid and, in doing so, reduced the computation to a standard setting where the Hilbert space has a finite number of dimensions. We verified that for small enough grid spacing, the entropy does not depend on the value of the spacing. As expected, $S_2[\text{particle 1}] \approx \ln(1.991)$, close to $\ln 2$, indicating two element-wise-distinct sets of particle momenta.

IV. GENERATING AN ENTANGLED STATE USING AN ADDITIONAL MIRROR. INTERFEROMETRIC MEASUREMENTS

The scheme described in the previous section is a preliminary, most obvious attempt to generate entanglement. We will now present a scheme that improves considerably on it by addressing the following two drawbacks of the original scheme.

The first drawback of the original scheme is that experimentally, it would require one to discard most of the repetitions, leaving only those where particles 2 through $(N - 1)$ were detected in positions close to the respective self-crossing values. Notice, however, the following: consider the N -body density corresponding to the *full* many-body wave function $\Psi(x_1, x_2, \dots, x_N)$ in Eq. (4): if this density is plotted as a function of the coordinate $\tilde{X} \equiv X_{\text{COM}} + \frac{1}{N}x_N$, then, in the vicinity of the self-crossing point, it shows interference

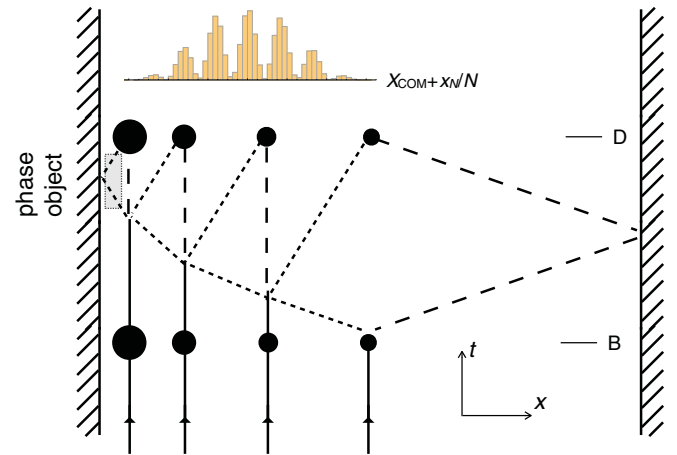


FIG. 2. A Galilean-cannon-based interferometer: an example with $N = 4$ particles. Initially all particles are at the point of self-crossing, $(x_1, x_2, x_3, x_4) = (1, 3, 6, \dots, \frac{N(N+1)}{2} \stackrel{N=4}{=} 10) \ell$. At time B, a beam splitter is applied to the lightest particle. After a series of collisions, each particle returns to its initial position, at the detection time D, where the particle positions are measured. A phase object, both spatially and temporarily localized, is shown as a gray rectangle. While no individual particle position distribution possesses any structure, the distribution of the $\tilde{X} \equiv X_{\text{COM}} + \frac{1}{N}x_N$ variable shows interference fringes, whose position is controlled by the phase introduced by the object. The inset shows a sample histogram derived from 79 900 simulated realizations of the detection cycle. These were selected from a longer sequence, such that we kept only the realizations with particle positions within a hypercube of dimensions $0.1\ell \times 0.1\ell \times 0.1\ell \times 0.1\ell$, centered at the self-crossing point $(1, 3, 6, 10) \ell$. The distance between the crests is consistent with the predicted value of $\Delta\tilde{X} = 2\pi/(M\mathcal{V}_x) = 0.0165 \ell$. The velocity kick induced by the beam splitter is the same as the initial velocity $\mathcal{V}_x^{(0)}$ of Fig. 1. The initial wave packet width of the lightest particle is $\sigma_{x,4} = 0.408 \ell$. The period of time between the beam splitting and detection is $0.0210 m_1 \ell^2 / \hbar$. The remaining parameters are the same as in Fig. 1. Note that because of the presence of the beam splitter and the additional mirror, the initial wave packet is no longer required to be long enough to self-cross. Accordingly, if viewed in the z coordinates, the initial many-body wave packet is perfectly round.

fringes with crest-to-crest distance of $\Delta\tilde{X} = 2\pi/(M\mathcal{V}_x)$. This is as if the fringes were produced by a wave for a single massive particle of mass M split by a $\pm M\mathcal{V}_x/2$ beam splitter. Here $X_{\text{COM}} \equiv \sum_{i=1}^N m_i x_i / M$ is the center-of-mass coordinate. These fringes can be made visible if the full four-body density distribution is used to produce the distribution of \tilde{X} .

The second drawback of the original scheme is that one needs a long coherence length in the initial wave packet for the lightest particle, to ensure interference at the self-crossing moment. This requirement can be relaxed if instead the lightest particle, like the other particles, starts at rest at its self-crossing position $x_N = \frac{N(N+1)}{2}\ell$. The lightest particle is then beam split and subsequently reflected from a second wall placed symmetrically to the first one (where the axis of symmetry coincides with the initial position of the lightest particle).

Both improvements are implemented in the interferometric scheme shown in Fig. 2. Indeed, in this scheme, the *beam splitter only acts on the lightest particle*, while due to the entanglement buildup, the more massive particles also affect the position of the fringes.

Below we will suggest a possible experimental realization in which the role of the particles is played by polymers of atoms: bosonic solitons. Assume that the lightest particle is a polymer consisting of $\mathcal{N}_{\text{light}}$ atoms. The heaviest one will contain $\mathcal{N}_{\text{heavy}} = \mathcal{N}_{\text{light}} \times N(N+1)/2 \sim \mathcal{N}_{\text{total}}$ atoms, where $\mathcal{N}_{\text{total}}$ is the total number of atoms in the system. Imagine that a phase object, a potential barrier of height U , *per atom*, acting during a limited time τ , is introduced between the wall and the default position of the heavy polymer. The best sensitivity to the strength U of the phase object can be easily estimated as $\Delta U_{\text{Galilean cannon}} \sim \hbar/(\tau\mathcal{N}_{\text{heavy}}) \sim \hbar/(\tau\mathcal{N}_{\text{total}})$, i.e., by the energy-time uncertainty relation for an interferometer formed by the heaviest polymer attempting to measure a barrier of height $\mathcal{N}_{\text{total}}U$ within a time τ . However, if $\mathcal{N}_{\text{total}}$ individual atoms are used, the maximal sensitivity is only $\Delta U_{\text{individual atoms}} \sim \hbar/(\tau\sqrt{\mathcal{N}_{\text{total}}})$, which is the sensitivity of a single-atom interferometer further improved by the signal-to-noise reduction using $\mathcal{N}_{\text{total}}$ repetitive measurements. The net relative sensitivity gain produced by the entanglement, for a given number of atoms $\mathcal{N}_{\text{total}}$ available, becomes a *gain* $\sim \sqrt{\mathcal{N}_{\text{total}}}$.

V. CONCLUSION AND OUTLOOK

In conclusion, we showed that for a particular one-dimensional mass sequence, it is possible to realize a protocol in which the system evolves, on its own, from a product state to a state where a heavy particle becomes entangled with a light one, thus realizing Schrödinger's a-cat-and-an- α -particle paradigm. We show numerically that the Rényi entropy of the heavy particle can rise to almost $\ln 2$. The robustness of the protocol is due to the integrability of the model that protects it from both classical stochastization and quantum diffraction. We suggest a concrete way to exploit the heavy-light entanglement by proposing an atomic interferometric sensor scheme that shows an $\sqrt{\mathcal{N}_{\text{total}}}$ increase in sensitivity, where $\mathcal{N}_{\text{total}}$ is the total number of atoms employed.

ACKNOWLEDGMENTS

The authors thank R. Hulet, H. Perrin, and C. Fuchs for help and comments. This work was supported by the US National Science Foundation Grant No. PHY-1402249, the Office of Naval Research Grant No. N00014-12-1-0400, and a grant from the Institut Francilien de Recherche sur les Atomes Froids (IFRAF). Financial support for T.S. provided by the Ecole Normale Supérieure is also appreciated.

APPENDIX A: A POTENTIAL EXPERIMENTAL REALIZATION USING ATOMIC SOLITONS: REALIZING DESIRED SOLITON MASS SPECTRA USING THE CONSERVATION LAWS GOVERNING THE NONLINEAR SCHRÖDINGER EQUATION

As an empirical realization of the scheme presented above we suggest using chains of cold bosonic solitons [21–23]. For our scheme, it is necessary to have two internal states available (or, alternatively, two kinds of atoms). We assume that like species attract each other, while the scattering length between the opposite species is tuned to a positive value. For ${}^7\text{Li}$ atoms, the desired window in Feshbach magnetic field strength does exist: in particular, at 855 G, the scattering lengths governing a $(m_F = -1)-(m_F = 0)$ mixture are $a_{-1,-1} \approx -0.5 a_B$, $a_{0,0} \approx -10 a_B$, and $a_{-1,0} \approx +1.0 a_B$, where a_B is the Bohr radius [24]. The kinetic energy of the relative motion of the solitons must be lower than both the intra- and interspecies interaction energy per particle, in order to ensure both a suppression of the inelastic effects and an absence of interspecies transmission.

Finally, the soliton sizes must be adjusted to fit the desired mass sequence. In order to accurately (and in the mean-field limit exactly) divide the gas onto the desired fractions, one can use the nontrivial integrals of motion present, at the mean-field level, in cold 1D Bose gases [25–27]. Let \tilde{N} be an integer and α a real number such that $-1/2 < \alpha \leq +1/2$. According to Ref. [26], a sudden increase in the coupling constant by a factor of $\eta = (\tilde{N} + \alpha)^2$ simultaneously produces two kinds of objects: first, \tilde{N} stationary solitons whose masses form the ratio $(1 + 2\alpha) : (3 + 2\alpha) : \dots : (2\tilde{N} - 1 + 2\alpha)$ and, second, spatially expanding thermal excitations that carry a fraction of $(\alpha/(\tilde{N} + \alpha))^2$ of the initial population. The most straightforward, but hopefully not the most optimal, way of generating the desired mass spectrum $1 : \frac{1}{3} : \frac{1}{6} : \frac{1}{10} : \dots : \frac{2}{N(N+1)}$ would be to start from a single soliton and then quench the coupling constant up by a factor $\eta = (\tilde{N} + \alpha)^2$, with $\alpha = \frac{1}{2}$ and $\tilde{N} = \text{lcm}(\{1, 3, 6, 10, \dots, \frac{N(N+1)}{2}\})$. Here $\text{lcm}(\dots)$ stands for the “least common multiple.” The resulting ensemble of \tilde{N} solitons (with masses increasing in a geometric progression) must subsequently be pruned extensively, leaving only the following members of the mass progression: $\frac{2\tilde{N}}{N(N+1)}, \frac{2\tilde{N}-1}{(N-1)N}, \dots$, and \tilde{N} . Those will constitute the desired sequence. Regretfully, only a fraction of $\frac{16\tilde{N}N}{(2\tilde{N}+1)(N+1)}$ of the initial soliton will be used; the rest will be lost to either a thermal component or the removed solitons of unwanted masses.

For instance, the $1, \frac{1}{3}, \frac{1}{6}, \frac{1}{10}$ mass spectrum considered above can be created using a quench of the coupling constant by a factor of $\frac{81}{4}$. The third, fifth, 10th, and 30th members of

the resulting arithmetic progression of masses would constitute the target sequence. This sequence will comprise $\frac{384}{3721} \approx 0.1$ of the population of the initial soliton. Note that already for a 10-soliton target sequence, this proportion is much lower, namely, $\frac{201600}{768453841} \approx 0.0003$. Further optimization of the mass-spectrum generating procedure is needed.

APPENDIX B: SENSITIVITY TO SHOT-TO-SHOT MASS FLUCTUATIONS

Potentially, residual fluctuations in the soliton occupations may be detrimental to the effects we discuss. To address this problem, we performed a series of classical simulations of the dynamics of a Galilean cannon with masses fluctuating from one run to another. For a given particle, the variance of its mass fluctuations was proportional to the mean particle mass, mimicking the Poissonian law, while the mass distribution itself had a rectangular profile. The spectra of the mean masses was the same as the mass spectra considered above. The parameter $\epsilon \equiv \text{s.d.}[m_N]/\text{mean}[m_N]$ controlled the overall magnitude of the mass fluctuations. In the integrable limit, $\epsilon \rightarrow 0$, the final velocities of the particles are equal. On the other hand, for finite values of ϵ , one expects to see, on average, an equipartition of energy. As a quantitative definition of the critical value ϵ^* that signifies the transition between the integrable and stochastic regimes, we choose the value of ϵ at which $S^E = S^v$, where S^E is the spectral entropy of the heaviest-lightest pair,

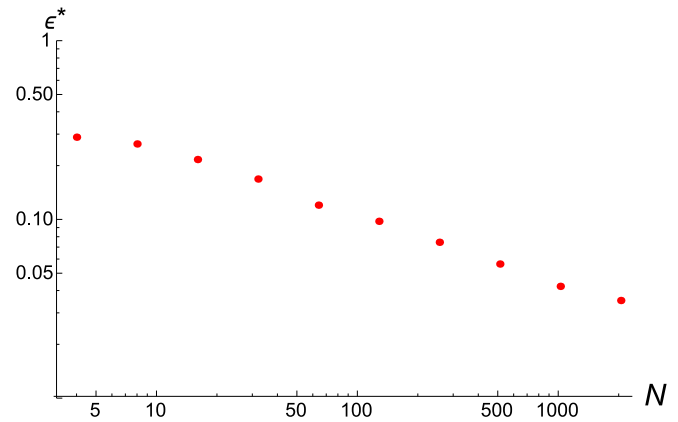


FIG. 3. Relative size of the mass fluctuation of the lightest particle at which a transition from an integrable to stochastic behavior occurs, as a function of the number of particles.

$S^E \equiv -\sum_{n=1, N} q_n^E \ln q_n^E$, with $q_n^E = \langle E_n \rangle_\infty / \sum_{n'=1, N} \langle E_{n'} \rangle_\infty$ and $E_n = m_n v_n^2 / 2$, where $\langle \dots \rangle_\infty$ is the infinite time average (this entropy is expected to be maximized whenever a system is stochastic); and S^v is the “velocity” entropy of the pair, $S^v \equiv -\sum_{n=1, N} q_n^v \ln q_n^v$, with $q_n^v = \langle v_n \rangle_\infty / \sum_{n'=1, N} \langle v_{n'} \rangle_\infty$ (in our case, this entropy is maximized in the integrable regime, because then all final velocities are equal). Our results (see Fig. 3) show that up to 1000 particles, mass fluctuations less than 5% can be tolerated.

-
- [1] Z. Hwang, F. Cao, and M. Olshanii, *J. Stat. Phys.* **161**, 467 (2015).
- [2] S. Redner, *Am. J. Phys.* **72**, 1492 (2004).
- [3] M. Gaudin, *La Fonction d'onde de Bethe* (Masson, Paris, 1983).
- [4] M. Olshanii and S. G. Jackson, *New J. Phys.* **17**, 105005 (2015).
- [5] B. Sutherland, *Beautiful Models: 70 Years of Exactly Solved Quantum Many-Body Problems* (World Scientific, Singapore, 2004).
- [6] S. Haroche and J.-M. Raimond, *Exploring the Quantum: Atoms, Cavities and Photons* (Oxford University Press, New York, 2006).
- [7] In the concrete scheme with four particles that we will actually propose, the mass ratio between the heaviest and the lightest particle will be 10. We do not mean to imply that this qualifies as an entanglement between something macroscopic and something microscopic, which is in the case of the original Schrödinger cat thought experiment. Nevertheless, we hope the analogy is clear.
- [8] As distinct from a subgroup thereof.
- [9] Another class of systems identified in Ref. [4], not considered here, corresponds to the cases where the system is bounded by two hard walls: a finite box.
- [10] E. Gutkin and B. Sutherland, *Proc. Natl. Acad. Sci. USA* **76**, 6057 (1979).
- [11] B. Sutherland, *J. Math. Phys.* **21**, 1770 (1980).
- [12] E. Gutkin, *Duke Math. J.* **49**, 1 (1982).
- [13] E. Emsiz, E. M. Opdam, and J. V. Stokman, *Comm. Math. Phys.* **264**, 191 (2006).
- [14] E. Emsiz, E. M. Opdam, and J. V. Stokman, *Sel. Math., New Ser.* **14**, 571 (2009).
- [15] E. Emsiz, *Lett. Math. Phys.* **91**, 61 (2010).
- [16] M. Girardeau, *J. Math. Phys.* **1**, 516 (1960).
- [17] E. H. Lieb and W. Liniger, *Phys. Rev.* **130**, 1605 (1963).
- [18] J. B. McGuire, *J. Math. Phys.* **5**, 622 (1963).
- [19] M. Gaudin, *Phys. Rev. A* **4**, 386 (1971).
- [20] J. Humphreys, *Introduction to Lie Algebras and Representation Theory* (Springer, New York, 1997).
- [21] L. Khaykovich, F. Schreck, G. Ferrari, T. Bourdel, J. Cubizolles, L. D. Carr, Y. Castin, and C. Salomon, *Science* **296**, 1290 (2002).
- [22] K. E. Strecker, G. B. Partridge, A. G. Truscott, and R. G. Hulet, *Nature (London)* **417**, 150 (2002).
- [23] S. L. Cornish, S. T. Thompson, and C. E. Wieman, *Phys. Rev. Lett.* **96**, 170401 (2006).
- [24] R. G. Hulet (private communication).
- [25] V. E. Zakharov and A. B. Shabat, *Zh. Eksp. Teor. Fiz.* **61**, 118 (1971) [*Sov. Phys. JETP* **34**, 62 (1972)].
- [26] J. Satsuma and N. Yajima, *Supp. Progr. Theor. Phys.* **55**, 284 (1974).
- [27] V. Dunjko and M. Olshanii, Superheated integrability and multisoliton survival through scattering off barriers, [arXiv:1501.00075](https://arxiv.org/abs/1501.00075).